Cell
P R E S S

Vesicular Glutamate Transport Promotes Dopamine Storage and Glutamate Corelease In Vivo

Thomas S. Hnasko,[1] Nao Chuhma,[2,3] Hui Zhang,[4] Germaine Y. Goh,[1] David Sulzer,[3,4] Richard D. Palmiter,[5] Stephen Rayport,[2,3] and Robert H. Edwards[1,*]
[1]Departments of Physiology and Neurology, University of California, San Francisco, San Francisco, CA 94158, USA
[2]Department of Psychiatry, Columbia University, New York, NY 10032, USA
[3]Department of Molecular Therapeutics, New York State Psychiatric Institute, New York, NY 10032, USA
[4]Departments of Neurology, Psychiatry and Pharmacology, Columbia University, New York, NY 10032, USA
[5]Howard Hughes Medical Institute & Department of Biochemistry, University of Washington, Seattle, WA 98195, USA
*Correspondence: robert.edwards@ucsf.edu
DOI 10.1016/j.neuron.2010.02.012

SUMMARY

Dopamine neurons in the ventral tegmental area (VTA) play an important role in the motivational systems underlying drug addiction, and recent work has suggested that they also release the excitatory neurotransmitter glutamate. To assess a physiological role for glutamate corelease, we disrupted the expression of vesicular glutamate transporter 2 selectively in dopamine neurons. The conditional knockout abolishes glutamate release from midbrain dopamine neurons in culture and severely reduces their excitatory synaptic output in mesoaccumbens slices. Baseline motor behavior is not affected, but stimulation of locomotor activity by cocaine is impaired, apparently through a selective reduction of dopamine stores in the projection of VTA neurons to ventral striatum. Glutamate co-entry promotes monoamine storage by increasing the pH gradient that drives vesicular monoamine transport. Remarkably, low concentrations of glutamate acidify synaptic vesicles more slowly but to a greater extent than equimolar Cl^-, indicating a distinct, presynaptic mechanism to regulate quantal size.

INTRODUCTION

For many neurons, the neurotransmitter they release is a defining feature. Release of a monoamine such as dopamine suggests a role for the cell in neuromodulation, glutamate a role in excitation, and GABA in inhibition. However, it has become clear that many neurons also release a classical transmitter other than the one with which they are usually associated. Inhibitory neurons in the spinal cord and brainstem release both glycine and GABA (Awatramani et al., 2005; Jonas et al., 1998; Nabekura et al., 2004), although this is not surprising since they are both inhibitory and a single carrier transports both into synaptic vesicles (Wojcik et al., 2006). On the other hand, seizure activity enables hippocampal mossy fibers to release GABA as well

as glutamate (Gutiérrez, 2000), transmitters with generally opposing actions in adulthood.

A number of observations suggest that neurons releasing the neuromodulatory monoamines can also release the excitatory transmitter glutamate. In single-cell (autaptic) cultures, serotonin, and dopamine neurons form glutamatergic synapses onto themselves (Johnson, 1994; Sulzer et al., 1998). Supporting the physiological relevance of these observations, stimulation of the ventral tegmental area (VTA) in horizontal brain slices elicits a monosynaptic excitatory postsynaptic current (EPSC) in nucleus accumbens (NAc) medium spiny neurons (Chuhma et al., 2009; Chuhma et al., 2004). In addition, stimulation of the VTA in anesthetized rats leads to monosynaptic glutamatergic EPSCs in pyramidal neurons of the prefrontal cortex (PFC) (Lavin et al., 2005). However, uncertainty has remained about the dopaminergic origin of this input to both striatum and cortex, which receive abundant glutamatergic input from other sources.

The corelease of glutamate predicts that dopamine neurons have the machinery required for exocytotic release of this excitatory transmitter. All cells contain glutamate for its role in protein synthesis and metabolism, but the vesicular glutamate transporters (VGLUTs) are specifically required for exocytotic release (Reimer and Edwards, 2004; Takamori, 2006). Indeed, the expression of three VGLUT isoforms appears to account for the glutamatergic phenotype of most neuronal populations demonstrated to use glutamate as a transmitter. In addition, the VGLUTs have a largely complementary distribution, with VGLUT1^{+} neurons in cerebral cortex and hippocampus and VGLUT2^{+} neurons in thalamus, midbrain, and hindbrain. VGLUT3 is generally expressed by populations considered to release a different transmitter, such as cholinergic interneurons of the striatum and serotonin neurons in the raphe (Fremeau et al., 2004).

In addition, several catecholamine populations express VGLUT2. Cultured dopamine neurons express high levels of VGLUT2, consistent with the corelease of glutamate in vitro (Dal Bo et al., 2004). In vivo, a subset of VTA dopamine neurons also expresses VGLUT2 mRNA by in situ hybridization (Bérubé-Carrière et al., 2009; Dal Bo et al., 2008; Kawano et al., 2006), but see also (Yamaguchi et al., 2007). Furthermore, single-cell RT-PCR detects VGLUT2 transcripts in 25% of dopamine neurons in the mouse midbrain at birth, with this proportion
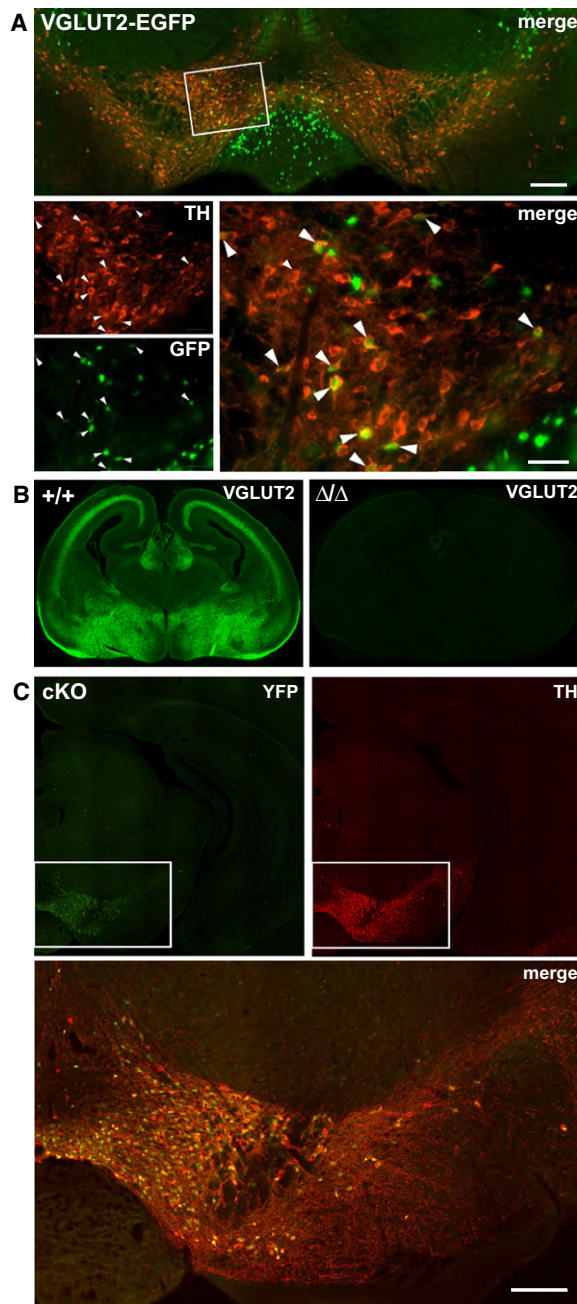
Figure 1. Histochemical Analysis of VGLUT2-EGFP BAC Transgenic Mice and the Conditional VGLUT2 Knockout

(A) Sections through the ventral midbrain of VGLUT2-EGFP BAC transgenic mice were immunostained for EGFP (green) and TH (red). The region of the VTA in the white box (above) is magnified in the images below. Many TH$^+$ neurons do not express EGFP and several EGFP$^+$ neurons do not contain TH, but a subset of TH$^+$ cells do also express EGFP. Size bar above indicates 200 μm, below 50 μm.

(B) Immunostaining of wild-type mouse brain (+/+, left) shows VGLUT2 immunoreactivity absent from the unconditional knockout (Δ/Δ).

(C) Immunofluorescence for YFP (green) and TH (red) in coronal brain sections from the VTA of a cKO mouse (with Cre recombinase under control of the DAT gene promoter both inactivating VGLUT2 and driving expression of YFP from the (Gt)Rosa26Sor floxed-stop reporter) shows that the vast majority of YFP$^+$

declining to 14% by 6 weeks of age (Mendez et al., 2008). Adrenergic and noradrenergic cell groups in the medulla also express VGLUT2 (Stornetta et al., 2002). However, the physiological role of glutamate release by catecholamine neurons remains unknown.

Previous work has suggested that uptake of an anion can promote filling with a cationic transmitter by influencing the H$^+$ electrochemical gradient ($\Delta\mu_H^+$) that drives uptake. $\Delta\mu_H^+$ produced by the vacuolar H$^+$-ATPase can be expressed as a chemical gradient (ΔpH), membrane potential ($\Delta\Psi$), or both. The entry of anions dissipates $\Delta\Psi$, thereby activating the H$^+$ pump to produce greater ΔpH. In particular, Cl$^-$ entry through the intracellular subset of ClC family carriers and perhaps even through the VGLUTs is generally thought to dissipate the $\Delta\Psi$ of endosomes and lysosomes as well as synaptic vesicles, thereby promoting ΔpH (Accardi and Miller, 2004; Jentsch et al., 2005; Picollo and Pusch, 2005; Schenck et al., 2009). The anions ATP and glutamate can also stimulate vesicle filling by serotonin and acetylcholine, respectively (Bankston and Guidotti, 1996; Gras et al., 2008). However, the relative role of different anions in vesicular monoamine transport remains unknown.

To determine whether dopamine neurons corelease glutamate in vivo and to assess its physiological role, we have generated a conditional knockout (cKO) mouse that lacks VGLUT2 specifically in these cells. We find that the loss of VGLUT2 in dopamine neurons reduces the locomotor response to cocaine, apparently by reducing vesicular storage of dopamine in the ventral striatum. We also find that glutamate stimulates vesicular monoamine transport despite substantial, physiological concentrations of Cl$^-$. Indeed, our observation that low concentrations of glutamate acidify synaptic vesicles to a greater extent and with different properties than equimolar Cl$^-$ suggests a presynaptic mechanism to regulate quantal size.

RESULTS

VGLUT2 localizes almost exclusively to synaptic vesicles and hence to nerve terminals, making it difficult to identify the cell bodies which express VGLUT2 by immunostaining. To circumvent this problem, we used bacterial artificial chromosome (BAC) transgenic mice expressing enhanced green fluorescent protein (EGFP) under the control of VGLUT2 regulatory sequences (Gong et al., 2003). Since EGFP is a soluble protein, it fills the cell bodies of neurons which express it, and the BAC transgenic mice exhibit appropriate expression of the EGFP reporter in the cell populations well established to express endogenous VGLUT2 (data not shown). We therefore used adult VGLUT2-EGFP mice to assess expression of VGLUT2 by mature midbrain dopamine neurons. Figure 1A shows that although many VTA neurons labeling for tyrosine hydroxylase (TH) do not express EGFP, and some EGFP$^+$ neurons do not contain TH (Yamaguchi et al., 2007), a substantial number of neurons

neurons coexpress TH, demonstrating the specificity of recombination. The merged image below shows a magnification of the boxed areas above. Size bar, 200 μm. See also Figure S1.
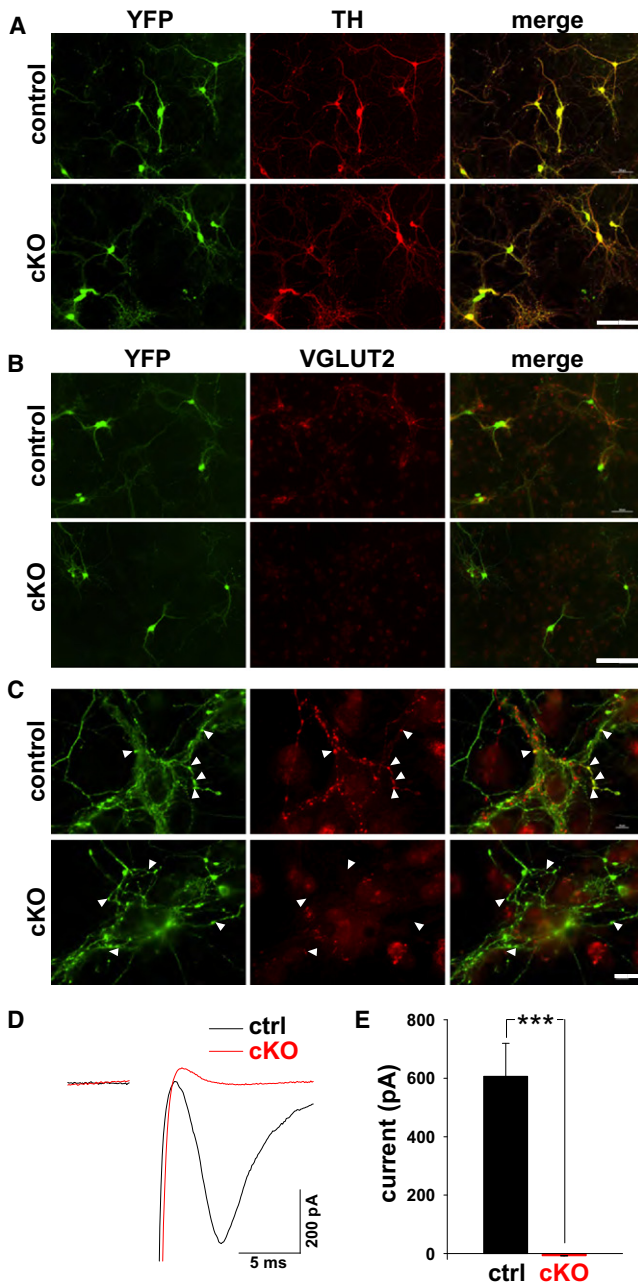
Figure 2. The Selective Deletion of VGLUT2 from Dopamine Neurons Eliminates Glutamatergic Currents Observed in Autaptic Cultures

(A) Postnatal midbrain cultures from control and cKO mice were grown on a glial monolayer and immunostained for YFP (green) and TH (red). The almost complete colocalization indicates that CreR has mediated recombination both efficiently and specifically in DA neurons of both cKO and control mice.

(B) Double staining of the cultures for YFP and VGLUT2 demonstrates that CreR has eliminated the expression of VGLUT2 by YFP$^+$ dopamine neurons of cKO but not control mice. Size bars in (A) and (B), 200 μm.

(C) Higher magnification images of double stained cultures show colocalization of VGLUT2 with YFP in the synaptic boutons of dopamine neurons from control but not cKO mice (arrowheads).

(D) A single YFP$^+$ dopamine neuron grown in microculture was recorded in whole-cell patch-clamp mode. From a holding potential of −60 mV, brief

express both TH and EGFP, consistent with previous reports indicating expression of VGLUT2 mRNA by a subset of VTA dopamine neurons in vivo (Kawano et al., 2006; Mendez et al., 2008).

To determine the function of VGLUT2 in midbrain dopamine neurons, we used homologous recombination in embryonic stem cells to produce a conditional allele of the mouse *Slc17a6* gene encoding VGLUT2, with exon 2 surrounded by loxP sites (see Figure S1A available online). After excision of the positive selectable marker at flanking FRT sites by crossing to mice that express germ line flp recombinase (Farley et al., 2000), the resulting VGLUT2$^{+/lox}$ animals were bred to mice expressing germ line Cre recombinase (Tallquist and Soriano, 2000), excising exon 2 to cause a frameshift that disrupts translation. Since VGLUT2 knockout mice die immediately after birth from respiratory failure (Moechars et al., 2006; Wallén-Mackenzie et al., 2006), we assessed the loss of VGLUT2 using brains from homozygous VGLUT2$^{Δ/Δ}$ embryos at 14.5–18.5 days gestation. Cre-mediated recombination eliminated VGLUT2 expression, as shown by western blot (Figure S1C) and immunohistochemistry (IHC) (Figure 1B). In addition, VGLUT2$^{lox/lox}$ mice show no difference from wild-type (WT) littermates in brain VGLUT2 expression (not shown), indicating that the residual FRT and loxP sites do not interfere with normal expression.

To disrupt VGLUT2 expression specifically in dopamine neurons, we crossed mice containing the conditional VGLUT2$^{+/lox}$ allele to mice that express Cre recombinase under the control of regulatory sequences from the *Slc6a3* gene that encodes the plasma membrane dopamine transporter (DAT) (Zhuang et al., 2005). To assess the specificity of recombination (Figure 1C) and identify the dopamine neurons with targeted disruption of the VGLUT2 gene, the mice carried one copy of the Cre-inducible floxed-stop yellow fluorescent protein (fsYFP) reporter (Srinivas et al., 2001). For all experiments, we compared control mice (*Slc17a6*$^{+/lox}$; *(Gt)Rosa26Sor*$^{+/fsYFP}$; *Slc6a3*$^{+/cre}$) to cKO littermates (*Slc17a6*$^{lox/lox}$; *(Gt)Rosa26Sor*$^{+/fsYFP}$; Slc6a3$^{+/cre}$). cKO mice were born at the expected Mendelian ratios and showed no obvious difference from littermate controls.

VGLUT2 Mediates Glutamate Corelease by Dopamine Neurons In Vitro and In Vivo

Previous work has shown that dopamine neurons grown in culture form glutamatergic synapses (Joyce and Rayport, 2000; Sulzer et al., 1998) and express VGLUT2 (Dal Bo et al., 2004). To determine whether the loss of VGLUT2 from dopamine neurons affects glutamate release, we first made postnatal (P1–P3) midbrain cultures, which contain a high proportion of tyrosine hydroxylase (TH)-positive dopamine neurons. Double staining for TH and YFP showed nearly complete colocalization (Figure 2A), indicating that Cre-mediated recombination had occurred in all dopamine neurons. We then double stained for YFP as well as the transporter, observing VGLUT2

depolarization to +20 mV induced an unclamped action potential followed by a fast EPSC in the control (ctrl) but not cKO cell.

(E) The mean excitatory autaptic current differs between control and cKO dopamine neurons. n = 8–11, ***p < 0.001 by two-tailed t test. Data indicate means ± SEM.
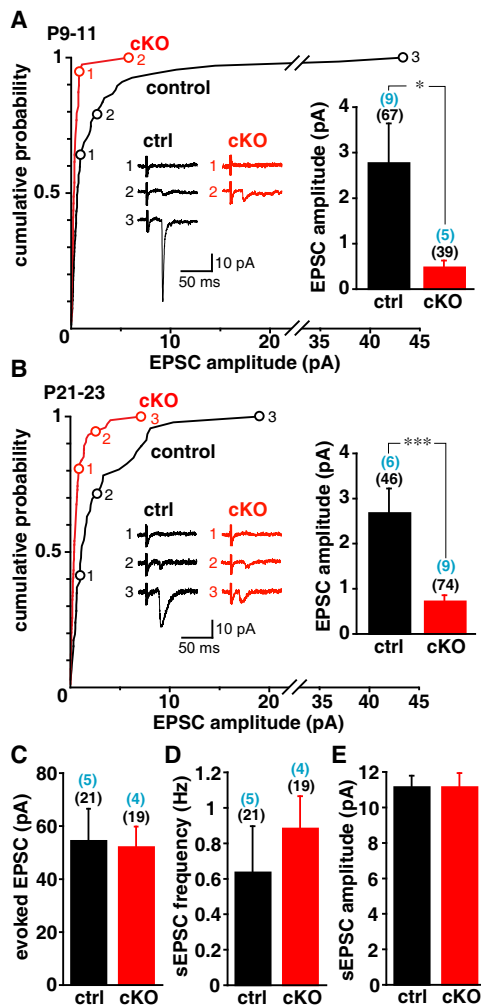
Figure 3. Mice Lacking VGLUT2 in Dopamine Neurons Show Reduced Glutamatergic Currents in NAc Neurons in Response to VTA Stimulation

(A and B) Glutamatergic responses evoked by stimulation in the VTA were recorded from medium spiny neurons in the medial shell of the NAc using 9–11 day (A) and 21–23 day (B) control and cKO mice. Cumulative probability plots of EPSC amplitudes show that at both ages, a larger proportion of cells from cKO mice show no or smaller responses than controls. Inset traces show representative examples of *No Response* (1), *Minimal Response* (2), and *Maximal Response* (3), with their location on the cumulative probability plot indicated with numbered open circles. Inset bar graphs of mean amplitudes from all recorded cells (including those without a response) show a major reduction in both younger and older cKO mice. The values in parentheses indicate the number of animals (above) and cells (below). *p < 0.05, ***p < 0.001 in unpaired t test.

(C–E) Glutamate input to YFP+ VTA dopamine neurons does not differ between P21–24 cKO mice and controls in terms of mean evoked EPSC amplitude (C), spontaneous EPSC frequency (D), or amplitude (E). Data in bar graphs indicate mean ± SEM.

immunoreactivity at synaptic boutons made by YFP+ dopamine neurons from control, but not cKO mice (Figures 2B and 2C). Conditional inactivation of the gene encoding VGLUT2 thus results in the loss of VGLUT2 specifically from dopamine neurons.

To determine whether VGLUT2 is required for glutamate release by dopamine neurons, we produced single-cell cultures of dopamine neurons that form synapses onto themselves (autapses), and examined the glutamatergic EPSCs evoked by brief depolarization. In autapses from control neurons, stimulation evoked EPSCs in 10/11 YFP+ dopamine neurons. However, EPSCs could not be evoked in any of the eight YFP+ cKO cells examined (Figures 2D and 2E). The cKO thus eliminates VGLUT2 from dopamine neurons, and at least in vitro, VGLUT2 is required for the corelease of glutamate by dopamine neurons.

We then used a mesoaccumbens slice preparation to assess a role for VGLUT2 in glutamate release by dopamine neurons in vivo. In this preparation, direct stimulation of the VTA elicits fast, glutamatergic EPSCs in MSNs of the NAc shell (Chuhma et al., 2004), enabling a distinction between glutamatergic input originating in the midbrain from abundant glutamatergic projections originating in cortex and thalamus (Fujiyama et al., 2006). Using this preparation, we observed a dramatic reduction in the glutamatergic EPSCs of postnatal day 9–11 (P9–11) cKO mice relative to control littermates (Figure 3A). Only 2.6% (1/39) of NAc neurons responded to VTA stimulation with an EPSC >2 pA in cKO mice, compared to 28% (19/67) of neurons from controls. Since dopamine neurons from older animals may express lower levels of VGLUT2 (Bérubé-Carrière et al., 2009; Mendez et al., 2008), we also examined mesoaccumbens slices from P21–23 mice. We again observed a major reduction in the evoked EPSC amplitude in cKO slices relative to controls (Figure 3B). VTA stimulation produced an EPSC >2 pA in 33% (15/46) of NAc neurons from control slices, but in only 5.4% (4/74) of cKO neurons. Since the cKO removes VGLUT2 selectively from dopamine neurons, dopamine neurons from wild-type mice must both express VGLUT2 and corelease glutamate in vivo.

In this mesoaccumbens slice preparation, only a minority of dopaminergic projections remain intact, so EPSCs <2 pA could reflect either defective glutamate release or the lack of intact dopamine neuron projections to the recorded MSN. Since we could not discriminate between these two possibilities, we included data from all recorded MSNs, including those without any EPSC (Figures 3A and 3B). It is also important to note that the littermate controls used for these experiments (*Slc17a6*+/lox; *Slc6a3*+/Cre) had undergone recombination of one VGLUT2 allele specifically in dopamine neurons and were therefore heterozygous for VGLUT2. Consistent with this, the mean evoked EPSC amplitude of NAc neurons from these control animals was ~50% that of age-matched mice wild-type at the VGLUT2 locus (*Slc17a6*+/+; *Slc6a3*+/Cre) (data not shown).

To assess the specificity of the cKO for VGLUT2 expressed by dopamine neurons, we examined synaptic input to the VTA, much of which depends on VGLUT2 (Geisler et al., 2007; Omelchenko and Sesack, 2007). Stimulating afferent projections to the VTA, we found that mean evoked EPSC amplitude in the midbrain does not differ between control and cKO animals (Figure 3C). We also observed no significant difference in the amplitude (Figure 3E) or frequency (Figure 3D) of spontaneous EPSCs recorded from VTA dopamine neurons. Although the cKO impairs glutamatergic transmission by dopaminergic efferents, it thus does not affect afferent inputs to these same cells.
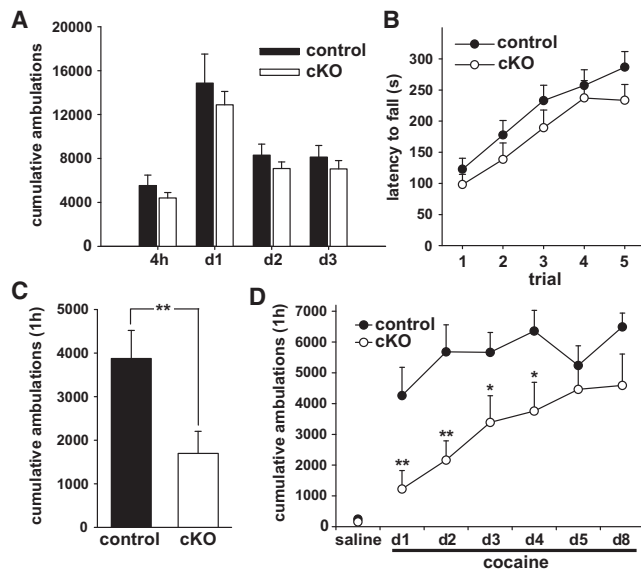
Figure 4. Conditional Knockout Mice Show Reduced Locomotor Response to Cocaine

(A) Spontaneous locomotor activity over a 72 hr period did not differ between cKO mice and control littermates (n = 8/genotype; two-tailed t test).

(B) Assessed on the rotarod, motor performance and learning showed no difference between genotypes by repeated-measures ANOVA (control n = 13, cKO n = 14).

(C) Naive cKO and control mice were injected with cocaine (20 mg/kg, i.p.) and locomotor activity monitored over the following hour. cKO mice exhibited substantially less locomotor activity than controls (control n = 15, cKO n = 16; $**p < 0.01$ by Mann-Whitney rank-sum test).

(D) To assess locomotor sensitization, naive mice were injected daily with cocaine (20 mg/kg i.p.) over 5 consecutive days and again 72 hr after the fifth injection. cKO mice exhibited less locomotor activity than controls for the first few cocaine injections. By the fifth injection, however, their response did not differ significantly from control mice. (control n = 7, cKO n = 8) repeated-measures ANOVA revealed a significant effect of genotype ($p \leq 0.01$) and a significant effect of treatment ($p < 0.001$). $*p < 0.05$, $**p < 0.01$ by Tukey post hoc comparison across genotype. Data presented as mean ± SEM. See also Figure S1.

The Conditional Knockout Reduces Cocaine-Induced Locomotor Activity, Dopamine Storage, and Release in the Ventral Striatum

To assess the utility of glutamate corelease, we examined a series of behaviors in cKO mice and littermate controls. Monitoring spontaneous activity, cKO animals showed no significant difference in either novelty-associated locomotion over 4 hr or in total locomotor activity over the following 3 days (Figure 4A). The cKO mice also exhibited no significant difference in the ability to perform or learn an accelerating rotarod task performed daily for 5 days (Figure 4B). Thus, the loss of VGLUT2 from dopamine neurons does not affect spontaneous activity, coordination or motor learning.

Cocaine increases extracellular dopamine by inhibiting its reuptake, stimulating locomotor activity through a mechanism that depends first on exocytotic dopamine release (Torres et al., 2003; Uhl et al., 2002). When challenged with 20 mg/kg cocaine, cKO mice showed significantly less locomotor activity than littermate controls (Figure 4C). However, repeated daily

injections with cocaine still elicited behavioral sensitization in cKO mice, and after several days, locomotor responses became indistinguishable from controls (Figures 4D and S2A). Despite the initially reduced effect of cocaine on locomotion, cKO mice formed a conditioned place preference (CPP) to cocaine, suggesting that at least some forms of reward and associative learning remain intact (Figures S2B and S2C).

Since cocaine-induced locomotion involves the extracellular accumulation of dopamine released by exocytosis, the initially reduced locomotor response might result from reduced vesicular stores. We thus measured striatal dopamine content, which closely reflects vesicular stores. Although dopamine levels in the dorsal striatum did not differ between cKO and littermate controls (Figure 5A), the levels of dopamine and its metabolites 3,4-dihydroxyphenylacetic acid (DOPAC) and homovanillic acid (HVA) all showed a 30%–40% reduction in the ventral striatum (including olfactory tubercle and NAc core as well as shell) of cKO mice (Figure 5B).

To assess directly the vesicular release of dopamine, we used fast-scan cyclic voltammetry (FSCV) (Wightman and Zimmerman, 1990) to measure the kinetics and amount of dopamine release evoked by a single action potential in striatal slices. Due to the heterogeneity of dopaminergic innervation, the results from three sites in the ventral striatum (specifically, within the NAc shell) of each slice were measured and averaged. Relative to control littermates, cKO mice showed a 23% reduction in the dopamine release evoked by a single action potential in the ventral striatum, with no change in dorsal striatum (Figures 5C and 5D).

To assess a potential effect on dopamine reuptake, we examined the kinetics of release at higher time resolution by amperometry. Similar to FSCV, amperometry showed a reduction in dopamine release from the NAc shell of cKO mice (28.7 ± 5 pA) relative to control (52.7 ± 5.4 pA; n = 20/genotype and p < 0.001 by paired two-tailed t test). The rates of dopamine clearance did not differ significantly between genotypes, but a trend toward slower clearance (τ = 407 ± 34 ms for cKO mice and 354 ± 26 ms for control, n = 20/genotype, p = 0.057 by paired t test) argues against increased clearance as a mechanism for reduced release in the slice.

To determine whether changes in dopamine production or terminal density might account for these differences, we quantified expression of the biosynthetic enzyme TH by fluorescent western analysis. The ventral striatum of cKO and control mice showed no difference in the amount of TH protein (Figure S3A). We also assessed functional TH activity in vivo, administering the aromatic acid decarboxylase (AADC) inhibitor NSD-1015 and measuring the accumulation of L-dopa in the ventral striatum. NSD-1015 increased tissue L-dopa levels as anticipated, but cKO mice did not differ from controls in L-dopa accumulation (Figure S3B).

Glutamate Stimulates Monoamine Uptake by VMAT2

Previous work has shown that glutamate uptake increases ΔpH across the synaptic vesicle membrane (Cidon and Sihra, 1989; Maycox et al., 1988). Since uptake by the vesicular monoamine transporters (VMATs) depends predominantly on ΔpH (Johnson, 1988), transport of glutamate into the same vesicles might thus
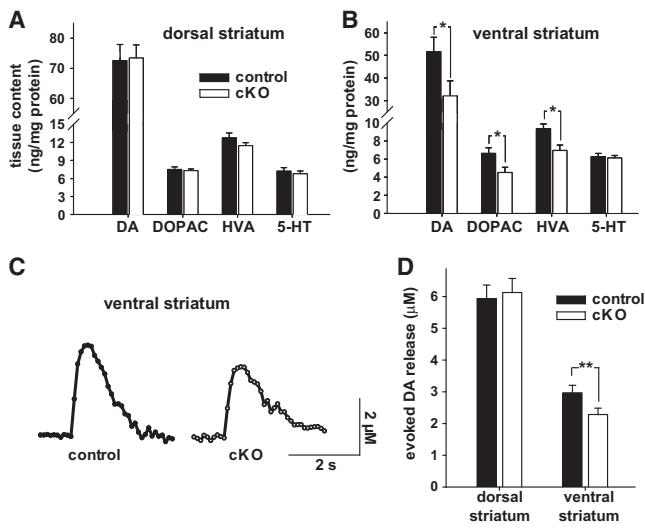
Figure 5. Reduced Dopamine Tissue Content and Evoked Dopamine Release in the Ventral Striatum of cKO Mice

(A and B) Tissue monoamine content was measured by HPLC coupled to an electrochemical detector. Punches from the dorsal striatum (A) showed no difference across genotype in the levels of dopamine (DA), dopamine metabolites dihydroxyphenylacetic acid (DOPAC) and homovanillic acid (HVA) and serotonin (5-HT) (n = 10/group). However, DA, DOPAC, and HVA were significantly reduced in the ventral striatum (B) of cKO mice relative to control littermates, with no change in 5-HT levels (n = 10/group; *p < 0.05 by two-tailed t test).

(C and D) The dopamine release evoked by single action potentials was measured in striatal slices using fast-scan cyclic voltammetry (FSCV). (C) The traces show representative examples of evoked dopamine release and reuptake in the ventral striatum. (D) The ventral striatum (NAc shell) of cKO mice released less dopamine than controls, but the two genotypes did not differ in the dorsal striatum. (n = 9 mice and 29 paired slices per genotype for dorsal striatum, 10 mice and 34 paired slices per genotype for ventral striatum). **p < 0.01 by two-tailed, paired t test. Data indicate mean ± SEM. See also Figure S2.

be expected to stimulate monoamine uptake. The loss of glutamate transport in VGLUT2 cKO mice may therefore account for the reduced dopamine content in ventral striatum (Figure 5B). However, this mechanism requires that VMAT2 and VGLUT2 localize to an overlapping population of synaptic vesicles.

To assess the colocalization of VGLUT2 with VMAT2 on synaptic vesicles, we performed immunoisolations using a light membrane fraction from the ventral striatum. We used rats for these experiments due to the greater availability of tissue and the limited cross-reactivity of several antibodies for mouse proteins. As anticipated, antibodies to the ubiquitous synaptic vesicle protein synaptophysin isolated significant amounts of VMAT2 (Figure 6A). Antibodies to VGLUT2 also precipitated most of the VMAT2 immunoreactivity, indicating that many of the VMAT2+ vesicles also contain VGLUT2. An antibody to Golgi matrix protein GM130, as well as controls lacking a primary antibody, failed to precipitate VMAT2, demonstrating the specificity of the immunoisolation. Reciprocal experiments using antibodies to VGLUT2 and synaptophysin also isolated large amounts of VGLUT2 (Figure 6B). VMAT2 antibodies isolated more VGLUT2 than negative controls, but the efficiency of
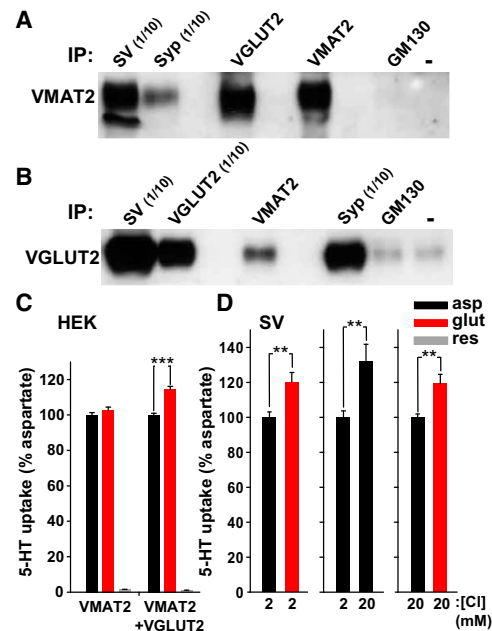
Figure 6. Glutamate Cotransport Stimulates Monoamine Uptake into Synaptic Vesicles

(A and B) Synaptic vesicles (SV) prepared from rat ventral striatum were immunoprecipitated (IP) with antibodies to synaptophysin (syp), VGLUT2, VMAT2, Golgi matrix protein GM130, or no primary antibody, and the isolated vesicles immunoblotted for VMAT2 (A) and VGLUT2 (B). Relative to the other samples, one-tenth of the indicated samples was immunoblotted to avoid saturation of the signal. Antibodies to VGLUT2 isolated SVs containing VMAT2 (A) and antibodies to VMAT2 isolated vesicles containing VGLUT2 (B), with minimal or no isolation in the absence of antibodies or with antibodies to GM130.

(C) The uptake of ^{3}H-5-HT was measured over 5 min in membranes from HEK293 cells transiently expressing VMAT2 with or without VGLUT2. (^{3}H-5-HT was used for these experiments because VMAT2 recognizes all the monoamine transmitters and 5-HT is more stable than the catecholamines.) Relative to aspartate, which is not recognized by the VGLUTs and has no effect on monoamine uptake (data not shown), equimolar glutamate (10 mM) stimulated transport in the presence, but not the absence, of VGLUT2, and reserpine (10 μM) largely eliminated the activity.

(D) Monoamine uptake was measured over 10 min using synaptic vesicles from rat ventral striatum. Glutamate (10 mM) stimulated monoamine uptake relative to aspartate in the presence of 2 mM Cl− (left). Increasing Cl− concentration from 2 to 20 mM also stimulated monoamine uptake in the absence of glutamate (middle). Despite the sensitivity of VMAT activity to Cl−, glutamate stimulates monoamine uptake even at higher, physiological concentrations of Cl− (20 mM) (right). **p < 0.01; ***p < 0.001 by two-tailed t test. Data presented as means ± SEM.

VGLUT2 immunoisolation by VMAT2 appears low, presumably because most VGLUT2 in the ventral striatum originates in the thalamus (Fujiyama et al., 2006), which does not express VMAT2.

To determine whether glutamate cotransport has the potential to stimulate monoamine uptake, we examined the effect of VGLUT2 coexpression on VMAT2 activity. In HEK293 cell membranes expressing both transporters, the addition of 10 mM glutamate stimulated monoamine uptake ∼15% relative to 10 mM aspartate (Figure 6C), which is not recognized by VGLUTs (Naito and Ueda, 1985; Takamori, 2006). We then examined the effect of glutamate on monoamine uptake by

synaptic vesicles from the ventral striatum (including olfactory tubercle, NAc core and shell). Again, glutamate stimulated monoamine uptake into native synaptic vesicles ~20% relative to aspartate (Figure 6D), providing additional functional evidence for the colocalization of a VGLUT with VMAT2. Since only a fraction of dopamine synapses are likely to contain VGLUT2 (Bérubé-Carrière et al., 2009; Kawano et al., 2006; Mendez et al., 2008), the effect of glutamate on monoamine storage that we observe may underestimate the full effect on those vesicles that contain both transporters.

Synaptic Vesicles Acidified with Glutamate or Chloride Differ in the Magnitude and Stability of ΔpH

Both glutamate and Cl⁻ appear to increase ΔpH by dissipating ΔΨ, thereby reducing the efflux of H⁺ driven by membrane potential and/or secondarily activating the H⁺ pump. Glutamate may thus stimulate monoamine uptake through a mechanism redundant with Cl⁻. Indeed, Cl⁻ occurs at substantially higher concentrations than glutamate in most cells. To determine whether glutamate and Cl⁻ differ in their uptake by synaptic vesicles, we monitored vesicle acidification using acridine orange, a dye quenched at low pH (Schuldiner et al., 1972). Since Cl⁻ and glutamate have both been shown to acidify synaptic vesicles from the whole brain, we used this mixed population due to the large amount of material required for these studies. Adding ATP to activate the H⁺ pump, we observed relatively little acidification in the absence of an anion. Because VGLUT activity depends on allosteric activation by low concentrations of Cl⁻, we then added 2 mM Cl⁻, a concentration that produces relatively little acidification on its own. The subsequent addition of either Cl⁻ or glutamate caused a greater increase in acidification (Figure 7A). At low concentrations, however, glutamate produced much more acidification than equimolar Cl⁻ (Figures 7A and 7B). Indeed, as little as 0.125 mM glutamate increased ΔpH more than 4 mM Cl⁻. On the other hand, increasing concentrations of Cl⁻ caused progressively greater increases in ΔpH, whereas the effects of glutamate saturated at 3–5 mM (Figure 7B), consistent with the known Km of VGLUTs (~1–3 mM; Fremeau et al., 2004; Takamori, 2006). High concentrations of Cl⁻ thus increase ΔpH more than high concentrations of glutamate. The kinetics of acidification also differed between the two anions. Although low concentrations of glutamate acidified to a greater extent than equivalent concentrations of Cl⁻, Cl⁻ acidified faster even at these low concentrations, and the difference in rate was more apparent at high concentrations (Figure 7C). Since recent work at the calyx of Held has demonstrated that the concentration of Cl⁻ at the nerve terminal can reach ~20 mM (Price and Trussell, 2006), we also tested the ability of 4 mM glutamate to acidify vesicles in the presence of 20 mM Cl⁻. We found that glutamate acidifies synaptic vesicles even after the addition of 20 mM Cl⁻ (Figure 7D). Glutamate also has a clear effect on peak ΔpH when added simultaneously with Cl⁻ (Figure 7E). However, the decline in ΔpH that followed this peak was less pronounced in vesicles acidified with glutamate than in those acidified with Cl⁻ (Figure 7E), suggesting that the anion responsible for acidification influences the stability of ΔpH.

To assess specifically the role of the anion in ΔpH stability, we took advantage of the vacuolar H⁺-ATPase inhibitor bafilomycin.
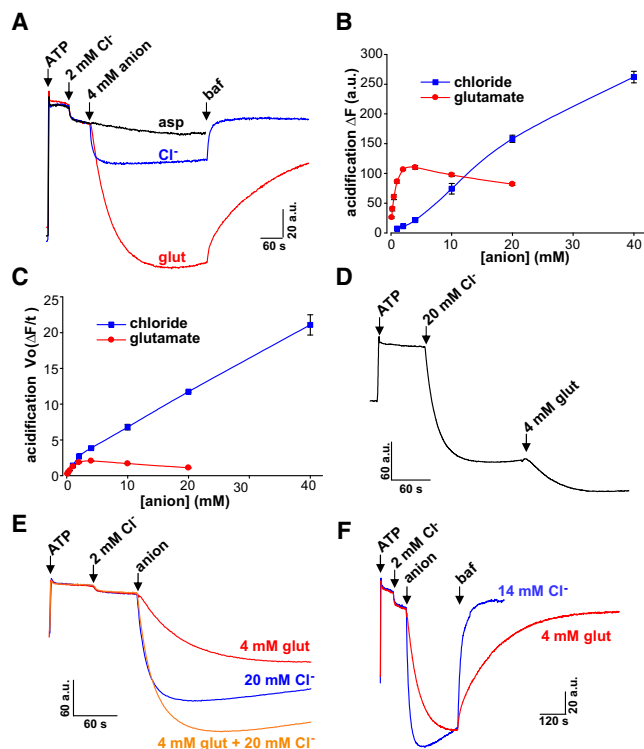
Figure 7. Chloride and Glutamate Acidify Synaptic Vesicles through Distinct Mechanisms

The quenching of acridine orange fluorescence was used to assess synaptic vesicle ΔpH in response to the addition of ATP and other anions.

(A) The traces show representative responses to the sequential addition of 1 mM ATP, 2 mM Cl⁻ (to provide allosteric activation of the VGLUTs) and either 4 mM Cl⁻ (Cl⁻, blue), glutamate (glut, red) or aspartate (asp, black). Bafilomycin (baf, 250 nM) inhibits the vacuolar H⁺-ATPase and allows dissipation of ΔpH. Under these conditions, glutamate produced greater acidification than equimolar Cl⁻, and aspartate had no effect. In addition, vesicles acidified with glutamate lost ΔpH more slowly in response to bafilomycin than those acidified with Cl⁻.

(B) Anion-induced acidification was fit to a single exponential and the maximum change in fluorescence (ΔF) extrapolated. Although glutamate produced greater acidification at low concentrations, Cl⁻ acidified to a greater extent at high concentrations (>10 mM).

(C) Fitting to a single exponential was also used to derive Initial rates of acidification (Vo ΔF/t). Cl⁻ acidifies more rapidly than glutamate, particularly at anion concentrations >4 mM. Data presented as means ± SEM. The sequential (D) or simultaneous (E) addition of 4 mM glutamate produced greater acidification than 20 mM Cl⁻ alone.

(F) Synaptic vesicles acidified to approximately the same extent with either 4 mM glutamate or 14 mM Cl⁻, but the vesicles acidified with glutamate lost ΔpH much more slowly in response to bafilomycin than those acidified with Cl⁻.

When bafilomycin inhibits the H⁺ pump, ΔpH immediately starts to collapse, enabling us to compare the rate of collapse for synaptic vesicles acidified with Cl⁻ versus glutamate. Since Cl⁻ and glutamate acidify to differing extents, we used concentrations of each that produce equivalent peak ΔpH (Figure 7F). After acidification with 14 mM Cl⁻, the addition of bafilomycin rapidly dissipated ΔpH, as anticipated. However, bafilomycin produced a much slower alkalinization of synaptic vesicles
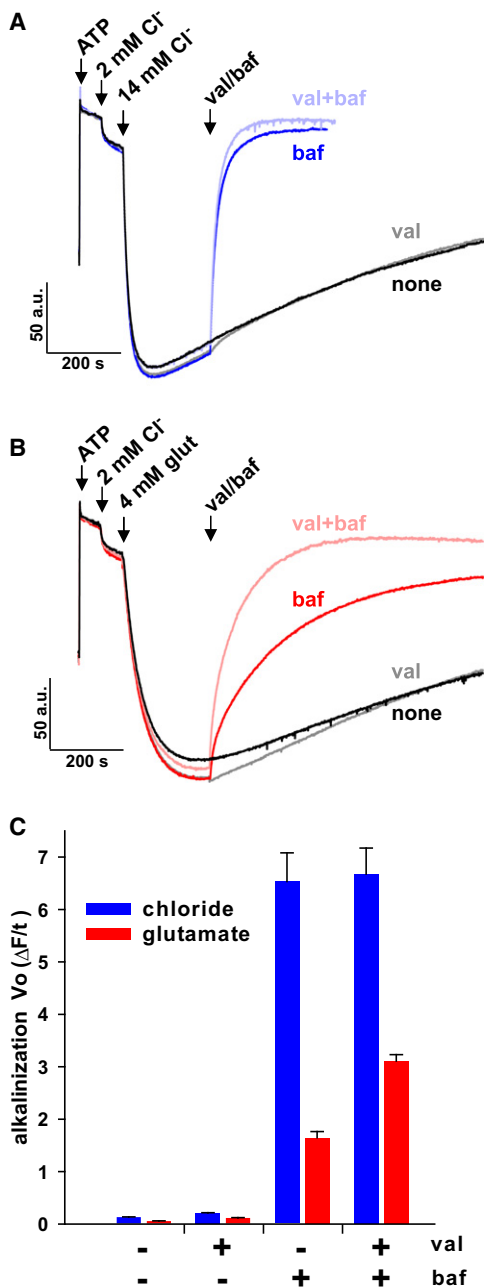
Figure 8. Membrane Potential Limits Proton Efflux in Vesicles Acidified by Glutamate

(A and B) Synaptic vesicles in 140 mM choline gluconate/10 mM K gluconate/10 mM HEPES (pH 7.4) were acidified by the sequential addition of ATP, 2 mM Cl^-, and then either 14 mM Cl^- (A) or 4 mM glutamate (B). The traces in black indicate vesicles without any further addition. At the arrow indicated baf/val, 250 nM bafilomycin (red) or 50 nM valinomycin (gray) or both (light red) were added. The potassium ionophore valinomycin accelerates the dissipation of ΔpH by bafilomycin to a much greater extent in vesicles acidified with glutamate than with Cl^-.

(C) Data from the first 60 s after baf/val addition were fit to either a straight line (no treatment or val) or single exponential (baf or val + baf) to derive initial rates of alkalinization (Vo ΔF/t). Within every condition tested, Cl^--acidified vesicles alkalinized significantly faster than those acidified by glutamate (p < 0.05 by

acidified with 4 mM glutamate (Figure 7F). For equivalent acidification, glutamate thus produces a more stable ΔpH than Cl^-. This effect presumably accounts for the slower decline in ΔpH observed after peak acidification even with an active H^+ pump (Figures 7E and 7F).

The differential stability of ΔpH in vesicles acidified with Cl^- and glutamate might reflect either differences in buffering by the two anions or differences in the mechanism of anion flux. The much higher pKa of glutamate (4.3) than Cl^- (-9) suggests that glutamate may delay alkalinization simply by acting as a buffer for vesicle pH after inhibition of the H^+ pump. On the other hand, dissipation of ΔpH requires a $\Delta\Psi$ sufficiently positive to promote H^+ efflux, and since anion efflux produces positive $\Delta\Psi$, differences in the mechanism of anion translocation may influence the rate of ΔpH collapse. To distinguish between these possibilities, we determined whether the imposition of a lumen-positive $\Delta\Psi$ accelerates dissipation of ΔpH. Synaptic vesicles were acidified in the presence of 10 mM K^+ gluconate with ATP, 2 mM Cl^- and then either 14 mM Cl^- or 4 mM glutamate (Figures 8A and 8B). In vesicles acidified with Cl^-, the K^+ iono-phore valinomycin had no clear effect on the dissipation of ΔpH by bafilomycin (Figure 8A), indicating that the development of $\Delta\Psi$ and hence anion efflux did not limit the rate of H^+ efflux. In contrast, valinomycin greatly accelerated the dissipation of ΔpH triggered by bafilomycin in vesicles acidified with glutamate (Figure 8B). Thus, $\Delta\Psi$ can limit the efflux of H^+ from vesicles acidified with glutamate, suggesting that the mechanism of anion flux contributes to the stability of ΔpH. Under all conditions, however, vesicles acidified with glutamate lost ΔpH more slowly than those acidified with Cl^- (Figure 8C), suggesting that glutamate may also act as a buffer to slow the dissipation of ΔpH.

The distinct roles of Cl^- and glutamate in synaptic vesicle acidification suggest that glutamate also has a specific role in the stimulation of monoamine uptake. However, the experiments demonstrating stimulation of monoamine uptake by glutamate were performed first with only 2 mM Cl^- (Figure 6D), a concentration sufficient to provide the well-established allosteric activation of VGLUTs (Hartinger and Jahn, 1993; Wolosker et al., 1996) but well below concentrations relevant for the nerve terminal. Consistent with previous results using synaptic vesicles (Erickson et al., 1990), we indeed found that 20 mM Cl^- produces a substantial increase in monoamine uptake relative to 2 mM (Figure 6D). Nonetheless, glutamate stimulated monoamine uptake at 20 mM Cl^- to the same extent it does at 2 mM (Figure 6D), supporting a role for glutamate distinct from Cl^-.

DISCUSSION

VGLUT2 Expression by Dopamine Neurons Confers Glutamate Release

Despite clear evidence for glutamate corelease by dopamine neurons in vitro (Joyce and Rayport, 2000; Sulzer et al., 1998),

two-tailed t test). The addition of val also accelerated alkalinization under each condition, with the exception of baf-treated vesicles acidified using Cl^- (p < 0.01 by two-tailed t test). Data presented as means ± SEM.

several factors complicate interpretation of the evidence for corelease in vivo. Stimulation of the VTA produces fast, glutamate-mediated responses in NAc and prefrontal cortex (Chuhma et al., 2004, 2009; Lavin et al., 2005), but it has remained unclear whether the released glutamate derives from dopamine neurons or from adjacent, nondopaminergic inputs. Inhibition of the glutamate response by activation of D2 autoreceptors in the VTA supports a dopaminergic origin for the released glutamate, but nondopamine neurons of the VTA also express D2 receptors (Margolis et al., 2006; Ungless et al., 2004). Loss of the glutamate response after lesion with 6-hydroxydopamine further supports a dopaminergic source for the released glutamate, but this toxin is also not entirely specific for dopamine neurons, particularly when administered locally at high concentrations (Poirier, 1975).

The results described here provide functional evidence using a conditional genetic approach that the glutamate released by VTA stimulation derives specifically from dopamine neurons. Taking advantage of the requirement for VGLUTs in exocytotic glutamate release, and the nonredundant expression of VGLUT isoforms by most neurons, we find that the loss of VGLUT2 indeed eliminates glutamate signaling by dopamine neurons in vitro. In vivo, the use of regulatory sequences from the dopamine transporter gene to drive expression of Cre recombinase ensures the inactivation of VGLUT2 selectively in dopamine neurons. Analysis of the cKO mice shows that the loss of VGLUT2 selectively in dopamine neurons greatly reduces VTA-evoked excitatory transmission in the NAc shell. Nonetheless, the cKO does not entirely eliminate the striatal glutamate response after VTA stimulation. Indeed, a distinct population of nondopaminergic midbrain neurons also express VGLUT2, although whether these cells project to nucleus accumbens remains unknown (Dal Bo et al., 2008; Kawano et al., 2006; Mendez et al., 2008; Yamaguchi et al., 2007). Incomplete excision by Cre recombinase or inadvertent stimulation of passing fibers are other possibilities. However, the striking effect of the cKO indicates that the expression of VGLUT2 by dopamine neurons accounts for essentially all of the glutamate release by these cells.

Despite the clear evidence for VGLUT2-dependent glutamate release by dopamine neurons, the level of VGLUT2 expression by these cells appears to be relatively low. In vitro, midbrain dopamine neurons express high levels of VGLUT2, but this apparently downregulates as a result of contact with GABAergic neurons (Mendez et al., 2008). In vivo, previous studies using in situ hybridization have indicated variable but generally low levels of VGLUT2 expression by dopamine neurons. One report described colocalization of VGLUT2 in 5.3%, 21.7%, 52.7% of TH+ neurons in, respectively, the paranigral, interfasicular, and rostral linear nuclei (Kawano et al., 2006), but another study described <1% colocalization throughout the VTA (Yamaguchi et al., 2007). These discrepancies may simply reflect differences in the regions examined or the ability to detect low abundance VGLUT2 transcripts. Indeed, sensitive single-cell RT-PCR shows that 25% of all midbrain dopamine neurons express VGLUT2 at birth, with this percentage declining to 14% by P45 (Mendez et al., 2008). Our results using adult VGLUT2-EGFP BAC transgenic mice now confirm the expression of VGLUT2 by a subset of midbrain dopamine neurons in a region of the VTA known to project to the striatum (Ikemoto, 2007). However, it is important to note that we used an amplification system to detect EGFP, and standard immunofluorescence suggested that midbrain dopamine neurons express lower levels of EGFP than other, known glutamatergic populations (data not shown).

VGLUT2 Facilitates Vesicle Filling with Dopamine

The cKO mice exhibit normal motor activity and learning, but show a greatly reduced locomotor response to acute administration of cocaine. Since cocaine blocks the reuptake of dopamine released by exocytosis, the reduced effect on locomotion may simply reflect a decrease in exocytotic release by the cKO. Indeed, we observed a decline in tissue dopamine content, suggesting a reduction in the storage pool (Fon et al., 1997). Consistent with the preferential expression of VGLUT2 by VTA rather than substantia nigra neurons (Kawano et al., 2006), the reduction in dopamine was also observed only in the ventral striatum (which receives projections from the VTA) rather than dorsal striatum (which receives projections from the substantia nigra). Depletion of monoamine stores might have resulted from increased release, but dopamine metabolites DOPAC and HVA were lower in the ventral striatum of cKO mice, indicating decreased rather than increased turnover. Further, we observed a reduction in the dopamine release evoked by stimulation of slices from the cKO ventral striatum. Thus, the blunted response to a single dose of cocaine appears to result from a reduction in dopamine stores and hence release. Although this mechanism appears to account for the observations, we cannot exclude the possibility that the loss of glutamate release from dopamine neurons contributes to the phenotype.

Despite the reduced dopamine stores and release, cKO mice increase their locomotor response to repeated administration of cocaine, indicating that locomotor sensitization does not require glutamate costorage and release. In addition to this form of plasticity, the cKO mice display normal CPP for cocaine, but this is not surprising since CPP has been shown to persist despite more severe, chronic reductions in dopamine storage (Hnasko et al., 2007; Spyraki et al., 1982; Torres et al., 2003; Uhl et al., 2002).

As predicted by a role for VGLUT2 in dopamine storage, immunoisolation experiments show that VMAT2 and VGLUT2 colocalize on a subpopulation of synaptic vesicles from the ventral striatum, presumably within dopaminergic projections. Serotonergic neurons also express VMAT2 and innervate the striatum, but this projection is much more sparse than the dopaminergic (Figures 5A and 5B; Zhou et al., 2005), and serotonergic neurons express VGLUT3 rather than VGLUT2 (Fremeau et al., 2002; Gras et al., 2002; Schäfer et al., 2002), effectively excluding them as a contaminant in these experiments. The ability of glutamate (but not aspartate) to stimulate monoamine uptake by synaptic vesicles from the ventral striatum provides additional, functional evidence for colocalization of a VGLUT with VMAT2. However, the expression of VGLUT2 by only a fraction of VTA dopamine neurons (Bérubé-Carrière et al., 2009; Kawano et al., 2006; Mendez et al., 2008) and the partial segregation of glutamate (or VGLUT2) and TH into different neuronal

processes (Descarries et al., 2008; Sulzer et al., 1998) suggest that the impact of VGLUT2 on monoamine storage by the entire ventral striatum reflects an even greater effect on the subset of dopamine neurons (and synaptic vesicles) that actually contain VGLUT2. Although the physiology (postsynaptic recording and electrochemistry) was performed in the NAc shell, the biochemical analysis was performed using the entire ventral striatum, and we do not know whether glutamate corelease and costorage also occur in olfactory tubercle or NAc core.

Glutamate and Chloride Acidify Synaptic Vesicles through Distinct Mechanisms

How does glutamate entry through VGLUT2 increase monoamine storage? The most likely explanation involves an increase in the driving force for monoamine uptake (ΔpH) due to the dissipation of $\Delta\Psi$ and resulting increase in ΔpH. Indeed, glutamate is well known to acidify synaptic vesicles (Cidon and Sihra, 1989; Maycox et al., 1988). Recent work using VGLUT3 knockout mice has invoked this mechanism to account for the increased storage of acetylcholine (ACh) by cholinergic interneurons of the striatum (Gras et al., 2008), since the vesicular ACh transporter, like VMAT2, depends primarily on ΔpH rather than $\Delta\Psi$ (Nguyen et al., 1998). However, the work on VGLUT3 showed an effect of glutamate on ACh uptake in the presence of 4 mM Cl^- (Gras et al., 2008), raising questions about the physiological relevance for the nerve terminal, which contains much higher Cl^- concentrations ($\sim$20 mM; Price and Trussell, 2006). We now find that glutamate stimulates monoamine uptake to the same extent in 2 and 20 mM Cl^-, showing that higher concentrations of Cl^- do not occlude the effect of glutamate. The two anions may therefore acidify synaptic vesicles through distinct, non-redundant mechanisms.

To assess differences in the acidification of synaptic vesicles by glutamate and Cl^-, we used the quenching of acridine orange fluorescence. Although we used a mixed population of synaptic vesicles from the whole brain, the properties observed should pertain to monoamine vesicles since the uptake of monoamine is stimulated by both anions. Remarkably, low concentrations of glutamate acidify to a much greater extent than equimolar Cl^-. This does not simply reflect the expression of VGLUTs on more synaptic vesicles than a Cl^- carrier because high concentrations of Cl^- acidify to a greater extent than glutamate. Indeed, the effect of glutamate saturates at $\sim$4 mM, as expected given the known VGLUT Km (1–3 mM).

How then can glutamate acidify to a greater extent than Cl^-? Although the identity of the Cl^- carrier on monoamine vesicles remains unknown, it may belong to the ClC family. In addition to plasma membrane Cl^- channels, the ClC family includes intracellular Cl^-/H^+ exchangers. Work on a bacterial member of the ClC family has shown that this protein exchanges 1 H^+ for 2 Cl^- (Accardi and Miller, 2004). Mammalian relatives include ClC-3, -5, and -7, which also behave as Cl^-/H^+ exchangers (Picollo and Pusch, 2005; Scheel et al., 2005) and in the case of ClC-7, have been shown to function with the same 2 Cl^-: 1 H^+ stoichiometry as the bacterial protein (Graves et al., 2008). Assuming that the ClC isoform on monoamine vesicles exhibits the same coupling stoichiometry, with the associated movement

of +3 charge, the concentration gradient of Cl^- at equilibrium is predicted by the equation:

$$2 \log_{10}\left(\left[Cl^-\right]_i / \left[Cl^-\right]_o\right) = \log_{10}\left(\left[H^+\right]_i / \left[H^+\right]_o\right) + 3\Delta\Psi/(2.3 \, RT/F) \tag{1}$$

where R is the gas constant, T the absolute temperature, F Faraday's constant, and the vacuolar H^+ pump determines ΔpH and $\Delta\Psi$. Assuming the H^+ pump can generate $\Delta\mu_{H^+} \sim 3$ in the form of ΔpH, $\Delta\Psi$, or a combination of both (Johnson et al., 1985; Johnson and Scarpa, 1979),

$$3 = \log_{10}\left(\left[H^+\right]_i / \left[H^+\right]_o\right) + \Delta\Psi/(2.3 \, RT/F) \tag{2}$$

and we can replace $\Delta\Psi$ in Equation 1 with 2.3 RT/F (3 − $\log_{10}([H^+]_i/[H^+]_o)$ to predict

$$\log_{10}\left(\left[H^+\right]_i / \left[H^+\right]_o\right) = 4.5 - \log_{10}\left(\left[Cl^-\right]_i / \left[Cl^-\right]_o\right) \tag{3}$$

Alternatively, Cl^- may actually enter through VGLUT2 itself. Previous work has shown that, like other members of the so-called type I phosphate transporter family (Bröer et al., 1998; Busch et al., 1996), the VGLUTs exhibit a Cl^- conductance (Bellocchio et al., 2000), a finding recently replicated with purified protein in a reconstituted system (Schenck et al., 2009). Although we still do not know whether this conductance is actually a channel, dependence on only $\Delta\Psi$ would generate a shallower Cl^- gradient, as predicted by the Nernst equation:

$$\log_{10}\left(\left[Cl^-\right]_i / \left[Cl^-\right]_o\right) = \Delta\Psi/(2.3 \, RT/F).$$

Replacing $\Delta\Psi$ with 2.3 RT/F (3 − $\log_{10}([H^+]_i/[H^+]_o)$ as above,

$$\log_{10}\left(\left[H^+\right]_i / \left[H^+\right]_o\right) = 3 - \log_{10}\left(\left[Cl^-\right]_i / \left[Cl^-\right]_o\right) \tag{4}$$

We do not know the stoichiometry of ionic coupling for the VGLUTs, but they have been repeatedly demonstrated to be driven by ΔpH (Bellocchio et al., 2000; Tabb et al., 1992; Takamori et al., 2000), strongly supporting a H^+ exchange mechanism despite the primary dependence on $\Delta\Psi$. Assuming the exchange of 1 H^+ for 1 glutamate and hence the movement of +2 charge,

$$\log_{10}\left(\left[glu^-\right]_i / \left[glu^-\right]_o\right) = \log_{10}\left(\left[H^+\right]_i / \left[H^+\right]_o\right) + 2\Delta\Psi/(2.3 \, RT/F). \tag{5}$$

Again replacing $\Delta\Psi$ with 2.3 RT/F (3 − $\log_{10}([H^+]_i/[H^+]_o)$,

$$\log_{10}\left(\left[H^+\right]_i / \left[H^+\right]_o\right) = 6 - \log_{10}\left(\left[glu^-\right]_i / \left[glu^-\right]_o\right) \tag{6}$$

For a particular anion gradient, glutamate flux through the VGLUTs is thus predicted to generate ΔpH 1.5 units greater than Cl^- flux through an intracellular ClC and 3 units greater than Cl^- flux through a channel, accounting for the greater acidification of synaptic vesicles by subsaturating concentrations of glutamate than equimolar Cl^-. Consistent with an effect of the anion on equilibrium rather than kinetics, even low concentrations of Cl^- acidify at least as rapidly as glutamate.

The anion used for acidification appears to influence the stability of ΔpH as well as its magnitude. After maximal acidification, synaptic vesicles acidified with Cl^- show a substantial, spontaneous decline in ΔpH. Despite equivalent peak ΔpH, vesicles acidified with glutamate show a much more stable ΔpH. Since these differences might simply reflect differences in the rate of acidification, with peak ΔpH achieved later in the case of glutamate, we acidified vesicles with ATP and either Cl^- or glutamate, then inhibited the pump with bafilomycin to assess the stability of preexisting ΔpH. Using concentrations of Cl^- and glutamate that produce equivalent acidification, vesicles acidified with glutamate retain ΔpH much longer than vesicles acidified with Cl^-. However, vesicles acidified with the two anions eventually return to a similar ΔpH, suggesting a difference in kinetics rather than thermodynamic equilibrium after inhibition of the H^+ pump.

The rate of ΔpH dissipation after inhibition of the H^+ pump might be controlled by buffering. The extremely low pK_a of HCl means that even high concentrations of Cl^- confer essentially no buffering beyond that provided by membrane protein and lipids. As a result, ΔpH might be expected to decline rapidly after inhibition of the H^+ pump in vesicles acidified with Cl^-. In contrast, the glutamate pK_a ~4.3 predicts protonation of up to 8% at a lumenal pH ~5.5 (Miesenböck et al., 1998; Mitchell and Ryan, 2004; Sankaranarayanan et al., 2000). With lumenal glutamate concentrations reaching 100 mM, this predicts low millimolar concentrations of protonated glutamate. Acidification with glutamate thus results in concentrations of bound H^+ that exceed those of free H^+ (low micromolar) by three orders of magnitude. However, we find that the imposition of positive $\Delta\Psi$ with K^+ and valinomycin greatly accelerates the dissipation of ΔpH after inhibition of the H^+ pump, indicating that $\Delta\Psi$ limits the rate of H^+ efflux after acidification with glutamate. On the other hand, even K^+ and valinomycin do not increase the loss of H^+ by glutamate-acidified vesicles to the same rate as Cl^--acidified vesicles, suggesting that glutamate may also act as buffer.

A rate-limiting role for $\Delta\Psi$ in the stability of ΔpH after inhibition of the H^+ pump suggests that the mechanism of anion efflux accounts for the differences between vesicles acidified with Cl^- and glutamate. In particular, Cl^- efflux through a channel will be opposed only by the development of $\Delta\Psi$, driving H^+ efflux. In contrast, glutamate efflux coupled to H^+ exchange will also be opposed by the outwardly directed ΔpH, limiting the development of $\Delta\Psi$ and hence H^+ efflux. The H^+ exchange mechanism that produces greater ΔpH at thermodynamic equilibrium thus also presents a kinetic barrier to the efflux of H^+, stabilizing the ΔpH that drives VMAT activity and "locking" monoamine inside synaptic vesicles.

EXPERIMENTAL PROCEDURES

BAC Transgenic Mice

Adult (2- to 3-month-old) hemizygous VGLUT2-EGFP BAC transgenic mice were perfused with cold PBS followed by 4% PFA, the brains removed, postfixed overnight in 4% PFA and then cryoprotected in 30% sucrose before freezing. Floating sections (30–40 μm) were rinsed with PBS containing 0.2% Triton X-100 (PBS-Tx), blocked for at least 1 hr in PBS-Tx containing 4% normal donkey serum, and incubated overnight at 4°C in blocking solution

with rabbit anti-TH (Millipore) and chicken anti-GFP (Invitrogen) antibodies (both at 1:1000). After washing the next day in PBS-Tx, the sections were incubated for two hours in blocking solution that contained cy3-conjugated donkey-anti-rabbit and HRP-conjugated donkey-anti-chicken secondary antibodies (Jackson Immunoresearch). The sections were then washed with PBS, incubated for 10 min with the FITC-conjugated TSA reagent (Perkin-Elmer), rinsed again with PBS, mounted, dehydrated through escalating alcohols followed by xylenes, coverslipped with DPX (Fluka), and imaged on a TE2000E Nikon inverted epifluorescence microscope with Photometrics Coolsnap HQ2 CCD camera.

Monoamine Levels and Release

To measure tissue monoamine content, mice were euthanized with CO_2, their brains rapidly removed, cooled, and after cutting 1-mm thick sections, punches made from ventral or dorsal striatum using a pipette tip cut to 1 mm in diameter. (The ventral striatum includes olfactory tubercle, NAc shell, and core.) Punches from each hemisphere were frozen on dry ice, stored at $-80°C$, and monoamine content determined by the Vanderbilt CMN/KC neurochemistry core using HPLC coupled to an electrochemical detector as previously described (Perez and Palmiter, 2005). To measure L-dopa accumulation, mice were treated with 100 mg/kg (i.p.) NSD-1015 (Sigma), tissue punches taken 30 min later and processed as described above.

Fast-scan cyclic voltammetry (FSCV) and amperometry were used to measure evoked dopamine release from coronal sections of the striatum (300 μm). Slices were allowed to recover for 1.5 hr in oxygenated artificial cerebrospinal fluid (ASCF, in mM: NaCl 125, KCl 2.5, NaHCO$_3$ 26, CaCl$_2$ 2.4, MgSO$_4$ 1.3, KH$_2$PO$_4$ 0.3, glucose 10) at room temperature, placed in a recording chamber, and superfused (1 ml/min) with ASCF at 36°C. Electrochemical recordings and electrical stimulation were performed as previously described (Zhang and Sulzer, 2003). Briefly, freshly cut carbon fiber electrodes ~5 μm in diameter were inserted into either the NAc shell or the dorsal striatum ~50 μm into the slice, and stimulation performed every 2 min with a single pulse using a bipolar stimulating electrode ~100 μm from the recording electrode. For FSCV, a triangular voltage wave (-400 to $+900$ mV at 280 V/s versus Ag/AgCl) was applied to the carbon fiber electrode every 100 ms and current recorded using an Axopatch 200B amplifier (Axon Instrument, Foster City, CA), with a low-pass Bessel Filter set at 10 kHz, digitized at 25 kHz (ITC-18 board, Instrutech Corporation, Great Neck, New York). Background-subtracted cyclic voltammograms identified the released substance as dopamine. The dopamine oxidation current was converted to concentration based upon a calibration of 5 μM dopamine in ASCF after the experiment. For amperometry, a constant voltage of 600 mV (relative to a reference electrode) was applied via the Axopatch 200B amplifier, and the current sampled at 5 kHz.

Immunoisolation

Ventral striata (including olfactory tubercle as well as NAc shell and core) from ~6-week-old mixed sex Spague-Dawley rats (Charles River) were dissected, homogenized on ice with a Teflon pestle in (mM) 150 NaCl, 10 HEPES-Tris (pH 7.4), 1 EGTA, 0.1 MgCl$_2$, 0.2 PMSF, and 1 μg/ml pepstatin A, sedimented at 20,000 × g for 10 min and the supernatant sedimented again at 27,000 × g for 10 min. The resulting supernatant (starting material) was frozen in liquid N$_2$, and stored at $-80°C$.

Primary antibodies were cross-linked to Protein G-coated Dynabeads (Invitrogen). Briefly, the beads were washed in citrate-phosphate buffer (pH 5.4) and incubated with constant mixing for 1 hr at RT in the same buffer containing a mouse antibody to p38 (Sigma), affinity-purified rabbit anti-VGLUT2 (Synaptic Systems), affinity-purified rabbit anti-VMAT2 (Pel-Freez), affinity-purified rabbit anti-golgi matrix protein 130 (Abcam), or no primary antibody. The beads were then washed in citrate-phosphate buffer, twice in 200 mM triethanolamine (pH 8.4), resuspended in 200 mM triethanolamine containing 20 mM dimethylpimelimidate, and cross-linked for 30 min at RT, again with constant mixing. The crosslinking was stopped by resuspension in 50 mM Tris (pH 7.5), and the beads were rinsed several more times with PBS containing protease inhibitors (PBS/PI). For immunoisolation, the beads were resuspended in PBS/PI containing 0.5% BSA, incubated with 300 μg synaptic vesicle protein for 1.5 hr at RT with constant mixing, washed in PBS/PI and resuspended in sample buffer for immunoblotting with rabbit anti-VMAT2

(1:1000) or anti-VGLUT2 (1:2000), followed by HRP-conjugated TrueBlot anti-rabbit antibody at 1:5000 (eBiosciences) and detection by enhanced chemiluminescence.

Vesicular Transport and Acidification

HEK293T cells were transfected by calcium phosphate with 18.75 μg VMAT2 cDNA ± 37.5 μg VGLUT2 cDNA per 15 cm plate. 48 hr after transfection, cells were harvested, pelleted, resuspended in 140 mM choline gluconate containing 10 mM HEPES-Tris (pH 7.4), and sonicated on ice. The lysate was centrifuged for 5 min at 16,000 rpm at 4°C, and the supernatant used for transport assays. Spun columns were prepared by swelling Sephadex G50-fine (Sigma) in choline gluconate buffer (140 mM choline gluconate, 10 mM HEPES-Tris, 2 mM KCl) for >3 hr before loading into 1 ml syringe barrels with Whatman GF/A filter paper support, and then prespinning at 2700 × g for 2 min. Uptake was performed by adding lysate (10–50 μg protein) to 160 μl reaction mix that contains 150 mM choline gluconate, 10 mM HEPES-Tris (pH 7.4), 2 mM MgATP, 2 mM KCl, 89 nM ^{H3}5-HT, and 10 mM K-aspartate or 10 mM K-glutamate ± 10 μM reserpine, incubating for 5 min at 30°C, transferring 140 μl to the top of the column, spinning again for 2 min, and measuring the radioactivity in 100 μl of the eluate using 5 ml Cytoscint (ICN) and a Beckman scintillation counter.

Ventral striata (olfactory tubercle, NAc shell, and core) were dissected from 3-week-old rat brains, and LP2 isolated from ventral striatum or the rest of the brain as previously described (Hell and Jahn, 1994). To measure transport, 30–100 μg ventral striatum LP2 was incubated for 10 min at 30°C in 200 μl reaction mix (described above), the entire reaction volume filtered through 200 μm DuraPore filters (Millipore), washed 3 times with 1.5 ml ice-cold choline gluconate buffer, and counts measured as above.

To measure acidification, 1.5 ml of 5 μM acridine orange in choline gluconate buffer was pre-incubated for >5 min at 30°C with constant stirring in a F4500 fluorescence spectrophotometer (Hitachi). For each run, 150 μg forebrain LP2 was added first, followed by 1 mM Mg^{2+}ATP, 2 mM choline Cl⁻, and variable concentrations of choline glutamate, choline aspartate, and/or choline Cl⁻, sometimes followed by addition of 250 nM bafilomycin (Calbiochem) and/or 50 nM valinomycin (Sigma). Acidification was replicated at least three times for each condition. To quantify the magnitude and rates of fluorescence change, curves were fit to linear or single exponential plots and values extracted using SigmaPlot and SigmaStat (Systat).

SUPPLEMENTAL INFORMATION

Supplemental Information includes three figures and Supplemental Experimental Procedures and can be found with this article online at doi:10.1016/j.neuron.2010.02.012.

REFERENCES

Accardi, A., and Miller, C. (2004). Secondary active transport mediated by a prokaryotic homologue of ClC Cl⁻ channels. Nature 427, 803–807.

Awatramani, G.B., Turecek, R., and Trussell, L.O. (2005). Staggered development of GABAergic and glycinergic transmission in the MNTB. J. Neurophysiol. 93, 819–828.

Bankston, L.A., and Guidotti, G. (1996). Characterization of ATP transport into chromaffin granule ghosts. Synergy of ATP and serotonin accumulation in chromaffin granule ghosts. J. Biol. Chem. 271, 17132–17138.

Bellocchio, E.E., Reimer, R.J., Fremeau, R.T., Jr., and Edwards, R.H. (2000). Uptake of glutamate into synaptic vesicles by an inorganic phosphate transporter. Science 289, 957–960.

Bérubé-Carrière, N., Riad, M., Dal Bo, G., Lévesque, D., Trudeau, L.E., and Descarries, L. (2009). The dual dopamine-glutamate phenotype of growing mesencephalic neurons regresses in mature rat brain. J. Comp. Neurol. 517, 873–891.

Bröer, S., Schuster, A., Wagner, C.A., Bröer, A., Forster, I., Biber, J., Murer, H., Werner, A., Lang, F., and Busch, A.E. (1998). Chloride conductance and Pi transport are separate functions induced by the expression of NaPi-1 in Xenopus oocytes. J. Membr. Biol. 164, 71–77.

Busch, A.E., Schuster, A., Waldegger, S., Wagner, C.A., Zempel, G., Broer, S., Biber, J., Murer, H., and Lang, F. (1996). Expression of a renal type I sodium/phosphate transporter (NaPi-1) induces a conductance in Xenopus oocytes permeable for organic and inorganic anions. Proc. Natl. Acad. Sci. USA 93, 5347–5351.

Chuhma, N., Zhang, H., Masson, J., Zhuang, X., Sulzer, D., Hen, R., and Rayport, S. (2004). Dopamine neurons mediate a fast excitatory signal via their glutamatergic synapses. J. Neurosci. 24, 972–981.

Chuhma, N., Choi, W.Y., Mingote, S., and Rayport, S. (2009). Dopamine neuron glutamate cotransmission: frequency-dependent modulation in the mesoventromedial projection. Neuroscience 164, 1068–1083.

Cidon, S., and Sihra, T.S. (1989). Characterization of a H+-ATPase in rat brain synaptic vesicles. Coupling to L-glutamate transport. J. Biol. Chem. 264, 8281–8288.

Dal Bo, G., St-Gelais, F., Danik, M., Williams, S., Cotton, M., and Trudeau, L.E. (2004). Dopamine neurons in culture express VGLUT2 explaining their capacity to release glutamate at synapses in addition to dopamine. J. Neurochem. 88, 1398–1405.

Dal Bo, G., Bérubé-Carrière, N., Mendez, J.A., Leo, D., Riad, M., Descarries, L., Lévesque, D., and Trudeau, L.E. (2008). Enhanced glutamatergic phenotype of mesencephalic dopamine neurons after neonatal 6-hydroxydopamine lesion. Neuroscience 156, 59–70.

Descarries, L., Berube-Carriere, N., Riad, M., Bo, G.D., Mendez, J.A., and Trudeau, L.E. (2008). Glutamate in dopamine neurons: synaptic versus diffuse transmission. Brain Res. Rev. 58, 290–302.

Erickson, J.D., Masserano, J.M., Barnes, E.M., Ruth, J.A., and Weiner, N. (1990). Chloride ion increases [3H]dopamine accumulation by synaptic vesicles purified from rat striatum: inhibition by thiocyanate ion. Brain Res. 516, 155–160.

Farley, F.W., Soriano, P., Steffen, L.S., and Dymecki, S.M. (2000). Widespread recombinase expression using FLPeR (flipper) mice. Genesis 28, 106–110.

Fon, E.A., Pothos, E.N., Sun, B.C., Killeen, N., Sulzer, D., and Edwards, R.H. (1997). Vesicular transport regulates monoamine storage and release but is not essential for amphetamine action. Neuron 19, 1271–1283.

Fremeau, R.T., Jr., Burman, J., Qureshi, T., Tran, C.H., Proctor, J., Johnson, J., Zhang, H., Sulzer, D., Copenhagen, D.R., Storm-Mathisen, J., et al. (2002). The identification of vesicular glutamate transporter 3 suggests novel modes of signaling by glutamate. Proc. Natl. Acad. Sci. USA 99, 14488–14493.

Fremeau, R.T., Jr., Voglmaier, S., Seal, R.P., and Edwards, R.H. (2004). VGLUTs define subsets of excitatory neurons and suggest novel roles for glutamate. Trends Neurosci. 27, 98–103.

Fujiyama, F., Unzai, T., Nakamura, K., Nomura, S., and Kaneko, T. (2006). Difference in organization of corticostriatal and thalamostriatal synapses between patch and matrix compartments of rat neostriatum. Eur. J. Neurosci. 24, 2813–2824.

Geisler, S., Derst, C., Veh, R.W., and Zahm, D.S. (2007). Glutamatergic afferents of the ventral tegmental area in the rat. J. Neurosci. 27, 5730–5743.

Gong, S., Zheng, C., Doughty, M.L., Losos, K., Didkovsky, N., Schambra, U.B., Nowak, N.J., Joyner, A., Leblanc, G., Hatten, M.E., and Heintz, N. (2003).

A gene expression atlas of the central nervous system based on bacterial artificial chromosomes. Nature *425*, 917–925.

Gras, C., Herzog, E., Bellenchi, G.C., Bernard, V., Ravassard, P., Pohl, M., Gasnier, B., Giros, B., and El Mestikawy, S. (2002). A third vesicular glutamate transporter expressed by cholinergic and serotoninergic neurons. J. Neurosci. *22*, 5442–5451.

Gras, C., Amilhon, B., Lepicard, E.M., Poirel, O., Vinatier, J., Herbin, M., Dumas, S., Tzavara, E.T., Wade, M.R., Nomikos, G.G., et al. (2008). The vesicular glutamate transporter VGLUT3 synergizes striatal acetylcholine tone. Nat. Neurosci. *11*, 292–300.

Graves, A.R., Curran, P.K., Smith, C.L., and Mindell, J.A. (2008). The Cl-/H+ antiporter ClC-7 is the primary chloride permeation pathway in lysosomes. Nature *453*, 788–792.

Gutiérrez, R. (2000). Seizures induce simultaneous GABAergic and glutamatergic transmission in the dentate gyrus-CA3 system. J. Neurophysiol. *84*, 3088–3090.

Hartinger, J., and Jahn, R. (1993). An anion binding site that regulates the glutamate transporter of synaptic vesicles. J. Biol. Chem. *268*, 23122–23127.

Hell, J.W., and Jahn, R. (1994). Preparation of synaptic vesicles from mammalian brain. In Cell Biology: A laboratory handbook (New York: Academic Press, Inc.).

Hnasko, T.S., Sotak, B.N., and Palmiter, R.D. (2007). Cocaine-conditioned place preference by dopamine-deficient mice is mediated by serotonin. J. Neurosci. *27*, 12484–12488.

Ikemoto, S. (2007). Dopamine reward circuitry: two projection systems from the ventral midbrain to the nucleus accumbens-olfactory tubercle complex. Brain Res. Rev. *56*, 27–78.

Jentsch, T.J., Poët, M., Fuhrmann, J.C., and Zdebik, A.A. (2005). Physiological functions of CLC Cl- channels gleaned from human genetic disease and mouse models. Annu. Rev. Physiol. *67*, 779–807.

Johnson, R.G., Jr. (1988). Accumulation of biological amines into chromaffin granules: a model for hormone and neurotransmitter transport. Physiol. Rev. *68*, 232–307.

Johnson, M.D. (1994). Synaptic glutamate release by postnatal rat serotonergic neurons in microculture. Neuron *12*, 433–442.

Johnson, R.G., and Scarpa, A. (1979). Protonmotive force and catecholamine transport in isolated chromaffin granules. J. Biol. Chem. *254*, 3750–3760.

Johnson, R.G., Carty, S.E., and Scarpa, A. (1985). Coupling of H+ gradients to catecholamine transport in chromaffin granules. Ann. N Y Acad. Sci. *456*, 254–267.

Jonas, P., Bischofberger, J., and Sandkühler, J. (1998). Corelease of two fast neurotransmitters at a central synapse. Science *281*, 419–424.

Joyce, M.P., and Rayport, S. (2000). Mesoaccumbens dopamine neuron synapses reconstructed in vitro are glutamatergic. Neuroscience *99*, 445–456.

Kawano, M., Kawasaki, A., Sakata-Haga, H., Fukui, Y., Kawano, H., Nogami, H., and Hisano, S. (2006). Particular subpopulations of midbrain and hypothalamic dopamine neurons express vesicular glutamate transporter 2 in the rat brain. J. Comp. Neurol. *498*, 581–592.

Lavin, A., Nogueira, L., Lapish, C.C., Wightman, R.M., Phillips, P.E., and Seamans, J.K. (2005). Mesocortical dopamine neurons operate in distinct temporal domains using multimodal signaling. J. Neurosci. *25*, 5013–5023.

Margolis, E.B., Lock, H., Hjelmstad, G.O., and Fields, H.L. (2006). The ventral tegmental area revisited: is there an electrophysiological marker for dopaminergic neurons? J. Physiol. *577*, 907–924.

Maycox, P.R., Deckwerth, T., Hell, J.W., and Jahn, R. (1988). Glutamate uptake by brain synaptic vesicles. Energy dependence of transport and functional reconstitution in proteoliposomes. J. Biol. Chem. *263*, 15423–15428.

Mendez, J.A., Bourque, M.J., Dal Bo, G., Bourdeau, M.L., Danik, M., Williams, S., Lacaille, J.C., and Trudeau, L.E. (2008). Developmental and target-dependent regulation of vesicular glutamate transporter expression by dopamine neurons. J. Neurosci. *28*, 6309–6318.

Miesenböck, G., De Angelis, D.A., and Rothman, J.E. (1998). Visualizing seCretion and synaptic transmission with pH-sensitive green fluorescent proteins. Nature *394*, 192–195.

Mitchell, S.J., and Ryan, T.A. (2004). Syntaxin-1A is excluded from recycling synaptic vesicles at nerve terminals. J. Neurosci. *24*, 4884–4888.

Moechars, D., Weston, M.C., Leo, S., Callaerts-Vegh, Z., Goris, I., Daneels, G., Buist, A., Cik, M., van der Spek, P., Kass, S., et al. (2006). Vesicular glutamate transporter VGLUT2 expression levels control quantal size and neuropathic pain. J. Neurosci. *26*, 12055–12066.

Nabekura, J., Katsurabayashi, S., Kakazu, Y., Shibata, S., Matsubara, A., Jinno, S., Mizoguchi, Y., Sasaki, A., and Ishibashi, H. (2004). Developmental switch from GABA to glycine release in single central synaptic terminals. Nat. Neurosci. *7*, 17–23.

Naito, S., and Ueda, T. (1985). Characterization of glutamate uptake into synaptic vesicles. J. Neurochem. *44*, 99–109.

Nguyen, M.L., Cox, G.D., and Parsons, S.M. (1998). Kinetic parameters for the vesicular acetylcholine transporter: two protons are exchanged for one acetylcholine. Biochemistry *37*, 13400–13410.

Omelchenko, N., and Sesack, S.R. (2007). Glutamate synaptic inputs to ventral tegmental area neurons in the rat derive primarily from subcortical sources. Neuroscience *146*, 1259–1274.

Perez, F.A., and Palmiter, R.D. (2005). Parkin-deficient mice are not a robust model of parkinsonism. Proc. Natl. Acad. Sci. USA *102*, 2174–2179.

Picollo, A., and Pusch, M. (2005). Chloride/proton antiporter activity of mammalian CLC proteins ClC-4 and ClC-5. Nature *436*, 420–423.

Poirier, L.J. (1975). Histopathologic changes associated with intracerebral injections of 6-hydroxydopamine (6-OHDA) and peroxide (H2O2) in the cat and the rat. J. Neural Transm. *37*, 209–218.

Price, G.D., and Trussell, L.O. (2006). Estimate of the chloride concentration in a central glutamatergic terminal: a gramicidin perforated-patch study on the calyx of Held. J. Neurosci. *26*, 11432–11436.

Reimer, R.J., and Edwards, R.H. (2004). Organic anion transport is the primary function of the SLC17/type I phosphate transporter family. Pflugers Arch. *447*, 629–635.

Sankaranarayanan, S., De Angelis, D., Rothman, J.E., and Ryan, T.A. (2000). The use of pHluorins for optical measurements of presynaptic activity. Biophys. J. *79*, 2199–2208.

Schäfer, M.K., Varoqui, H., Defamie, N., Weihe, E., and Erickson, J.D. (2002). Molecular cloning and functional identification of mouse vesicular glutamate transporter 3 and its expression in subsets of novel excitatory neurons. J. Biol. Chem. *277*, 50734–50748.

Scheel, O., Zdebik, A.A., Lourdel, S., and Jentsch, T.J. (2005). Voltage-dependent electrogenic chloride/proton exchange by endosomal CLC proteins. Nature *436*, 424–427.

Schenck, S., Wojcik, S.M., Brose, N., and Takamori, S. (2009). A chloride conductance in VGLUT1 underlies maximal glutamate loading into synaptic vesicles. Nat. Neurosci. *12*, 156–162.

Schuldiner, S., Rottenberg, H., and Avron, M. (1972). Determination of pH in chloroplasts. 2. Fluorescent amines as a probe for the determination of pH in chloroplasts. Eur. J. Biochem. *25*, 64–70.

Spyraki, C., Fibiger, H.C., and Phillips, A.G. (1982). Cocaine-induced place preference conditioning: lack of effects of neuroleptics and 6-hydroxydopamine lesions. Brain Res. *253*, 195–203.

Srinivas, S., Watanabe, T., Lin, C.S., William, C.M., Tanabe, Y., Jessell, T.M., and Costantini, F. (2001). Cre reporter strains produced by targeted insertion of EYFP and ECFP into the ROSA26 locus. BMC Dev. Biol. *1*, 4.

Stornetta, R.L., Sevigny, C.P., and Guyenet, P.G. (2002). Vesicular glutamate transporter DNPI/VGLUT2 mRNA is present in C1 and several other groups of brainstem catecholaminergic neurons. J. Comp. Neurol. *444*, 191–206.

Sulzer, D., Joyce, M.P., Lin, L., Geldwert, D., Haber, S.N., Hattori, T., and Rayport, S. (1998). Dopamine neurons make glutamatergic synapses in vitro. J. Neurosci. *18*, 4588–4602.

Tabb, J.S., Kish, P.E., Van Dyke, R., and Ueda, T. (1992). Glutamate transport into synaptic vesicles. Roles of membrane potential, pH gradient, and intravesicular pH. J. Biol. Chem. *267*, 15412–15418.

Takamori, S. (2006). VGLUTs: 'exciting' times for glutamatergic research? Neurosci. Res. *55*, 343–351.

Takamori, S., Rhee, J.S., Rosenmund, C., and Jahn, R. (2000). Identification of a vesicular glutamate transporter that defines a glutamatergic phenotype in neurons. Nature *407*, 189–194.

Tallquist, M.D., and Soriano, P. (2000). Epiblast-restricted Cre expression in MORE mice: a tool to distinguish embryonic vs. extra-embryonic gene function. Genesis *26*, 113–115.

Torres, G.E., Gainetdinov, R.R., and Caron, M.G. (2003). Plasma membrane monoamine transporters: structure, regulation and function. Nat. Rev. Neurosci. *4*, 13–25.

Uhl, G.R., Hall, F.S., and Sora, I. (2002). Cocaine, reward, movement and monoamine transporters. Mol. Psychiatry *7*, 21–26.

Ungless, M.A., Magill, P.J., and Bolam, J.P. (2004). Uniform inhibition of dopamine neurons in the ventral tegmental area by aversive stimuli. Science *303*, 2040–2042.

Wallén-Mackenzie, A., Gezelius, H., Thoby-Brisson, M., Nygård, A., Enjin, A., Fujiyama, F., Fortin, G., and Kullander, K. (2006). Vesicular glutamate transporter 2 is required for central respiratory rhythm generation but not for locomotor central pattern generation. J. Neurosci. *26*, 12294–12307.

Wightman, R.M., and Zimmerman, J.B. (1990). Control of dopamine extracellular concentration in rat striatum by impulse flow and uptake. Brain Res. Brain Res. Rev. *15*, 135–144.

Wojcik, S.M., Katsurabayashi, S., Guillemin, I., Friauf, E., Rosenmund, C., Brose, N., and Rhee, J.S. (2006). A shared vesicular carrier allows synaptic corelease of GABA and glycine. Neuron *50*, 575–587.

Wolosker, H., de Souza, D.O., and de Meis, L. (1996). Regulation of glutamate transport into synaptic vesicles by chloride and proton gradient. J. Biol. Chem. *271*, 11726–11731.

Yamaguchi, T., Sheen, W., and Morales, M. (2007). Glutamatergic neurons are present in the rat ventral tegmental area. Eur. J. Neurosci. *25*, 106–118.

Zhang, H., and Sulzer, D. (2003). Glutamate spillover in the striatum depresses dopaminergic transmission by activating group I metabotropic glutamate receptors. J. Neurosci. *23*, 10585–10592.

Zhou, F.M., Liang, Y., Salas, R., Zhang, L., De Biasi, M., and Dani, J.A. (2005). Corelease of dopamine and serotonin from striatal dopamine terminals. Neuron *46*, 65–74.

Zhuang, X., Masson, J., Gingrich, J.A., Rayport, S., and Hen, R. (2005). Targeted gene expression in dopamine and serotonin neurons of the mouse brain. J. Neurosci. Methods *143*, 27–32.